

# Synthesis, Characterization, and Electrochemical Properties of Dinuclear Complexes Assembled from Asymmetric Co<sup>III</sup> Bis(dioximates) and Boronic Acids

Renata Dreos,<sup>\*[a]</sup> Patrizia Siega,<sup>[a]</sup> Silvia Scagliola,<sup>[a]</sup> Lucio Randaccio,<sup>\*[a]</sup> Giorgio Nardin,<sup>[a]</sup> Claudio Tavagnacco,<sup>[a]</sup> and Manuela Bevilacqua<sup>[a]</sup>

**Keywords:** Boronic acid / Cobalt / Dioximes / Enantioselectivity / Electrochemistry

Bis(methylphenylglyoximate)cobalt(III) complexes exist both as *cis* and *trans* isomers due to the asymmetry of the equatorial ligand, and, when the axial ligands are different, the *trans* isomer is chiral. The reaction of racemic *trans*-[CH<sub>3</sub>Co(mpgH)<sub>2</sub>py] (**1**) with either 3- or 4-pyridylboronic acid affords dimeric units arranged on a crystallographic symmetry center such that the pyridyl nitrogen of one moiety coordinates to the Co atom of the symmetry-related unit. In principle, three structurally different dimeric species (two homodimers and one heterodimer) can be obtained. Time-resolved <sup>1</sup>H NMR spectra of a 1:1 mixture of racemic **1** and either 3- or 4-pyridylboronic acid in CDCl<sub>3</sub>/CD<sub>3</sub>OD show that the reaction does not converge toward a unique species in solution. Nevertheless, X-ray structures show that the heterochiral dimers are the only products that crystallize from the

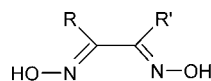
reaction mixture. The nature of the dioximate side groups does not affect the geometry of the dimeric arrangements assembled by 4-pyridylboronic acid ("molecular box"). On the contrary, the geometry of the species assembled by 3-pyridylboronic acid varies from the "molecular parallelogram" obtained from the bis(dimethylglyoximates) to the highly squeezed "molecular box" obtained from bis(methylphenylglyoximates). Cyclic voltammetry studies show that the metal centers in the dimeric species do not interact with each other and undergo a simultaneous redox process. However, depending on the geometry of the systems, the redox process involves a single four-electron reduction for **3** and **5** or two consecutive two-electron reduction steps for **4** and **6**.

(© Wiley-VCH Verlag GmbH & Co. KGaA, 69451 Weinheim, Germany, 2005)

## Introduction

Organobis(dimethylglyoximate)cobalt(III) complexes {organocobaloximes, [CH<sub>3</sub>Co(dmgh)<sub>2</sub>L], where L is a neutral ligand} have been extensively studied, mainly for their interest as vitamin B<sub>12</sub> models,<sup>[1]</sup> but also for their use as polymerization catalysts<sup>[2]</sup> and as templates in organic synthesis.<sup>[3]</sup> Some examples of cobalt complexes with dioximate ligands other than dmgh<sub>2</sub>, such as glyoximates (gH),<sup>[4]</sup> dicyclohexylglyoximates (chgH),<sup>[5]</sup> and diphenylglyoximates (dpgH),<sup>[6]</sup> are known. Derivatives containing mixed equatorial ligand sets, which include one dpgH and either a dmgh or chgH, have also been reported.<sup>[7]</sup> To the best of our knowledge, only two reports exist of cobalt complexes with the asymmetric methylphenylglyoximate ligand (mpgH).<sup>[8]</sup>

Organocobaloximes with either one or both of the intramolecular OHO bridges replaced by organoboryl groups are well known and have recently been reviewed.<sup>[9]</sup> We have used organobis(dimethylglyoximate)- and organobis(di-

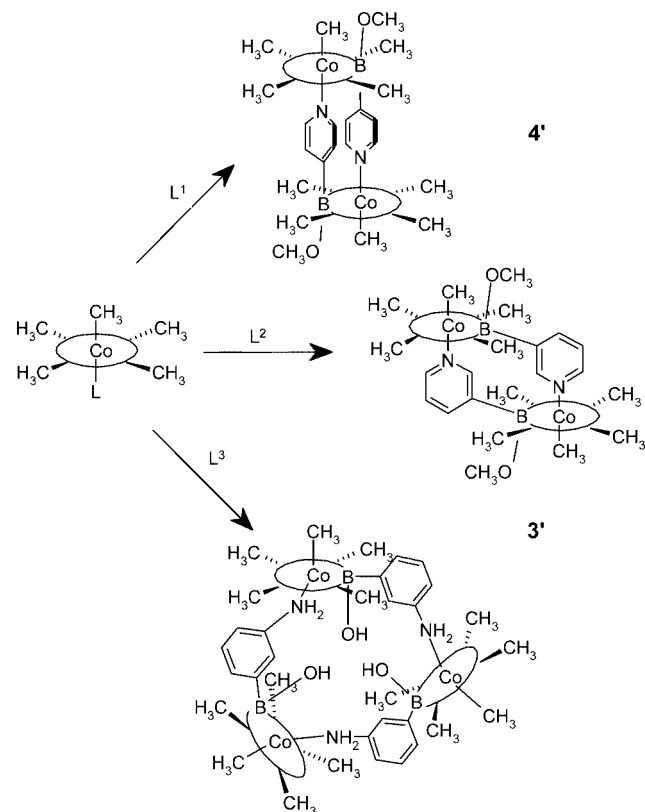


|  |                   |
|--|-------------------|
| R = R' = CH <sub>3</sub>                                 | dmgh <sub>2</sub> |
| R = R' = C <sub>6</sub> H <sub>5</sub>                   | dpgH <sub>2</sub> |
| R = CH <sub>3</sub> , R' = C <sub>6</sub> H <sub>5</sub> | mpgH <sub>2</sub> |
| R = R' = C <sub>6</sub> H <sub>11</sub>                  | chgH <sub>2</sub> |
| R = R' = H   | gH <sub>2</sub>   |

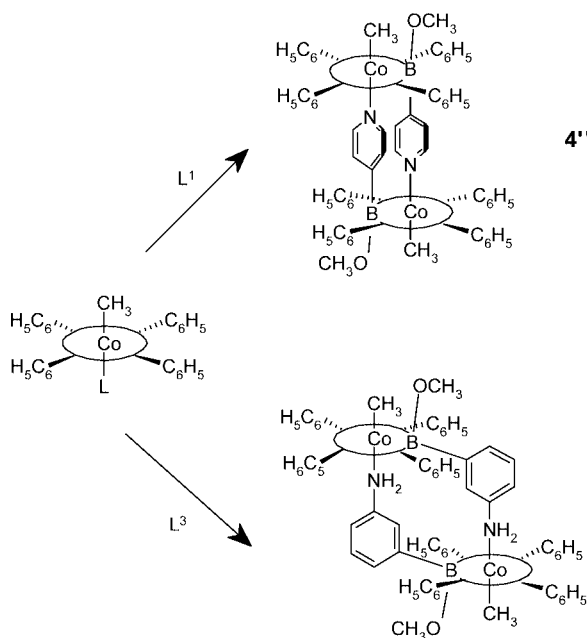
phenylglyoximate)cobalt(III) complexes as building blocks in the assembly of supramolecular systems.<sup>[10]</sup> Indeed, functionalized aromatic boronic acids have been shown to efficiently direct the assembly of organocobaloximes through the reaction of the B(OH)<sub>2</sub> group with the oxime bridge of one cobaloxime molecule, with simultaneous coordination of the donor atom to the cobalt of another cobaloxime.<sup>[10]</sup> Products of different nuclearity and geometry have been obtained, depending on the geometry of the boronic acid used as linker (L<sup>1</sup>, L<sup>2</sup>, and L<sup>3</sup>, Scheme 1). The most relevant consequence of replacing the methyl groups by phenyl groups in the equatorial ligand is a change of the nuclearity of the supramolecular species assembled with 3-aminophenylboronic acid (L<sup>3</sup>): a molecular triangle was obtained starting from [CH<sub>3</sub>Co(dmgh)<sub>2</sub>L] (Scheme 1), whereas a dimeric species was obtained from [CH<sub>3</sub>Co(dpgH)<sub>2</sub>L] (Scheme 2), the trimeric arrangement being prevented by the steric hindrance of the phenyl groups.<sup>[11]</sup>

[a] Dipartimento di Scienze Chimiche, Università di Trieste, Via Licio Giorgieri 1, 34127, Trieste, Italy  
Fax: +39-040-558-3903  
E-mail: dreos@univ.trieste.it  
randaccio@univ.trieste.it

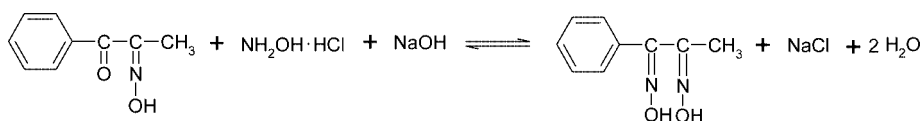
Supporting information for this article is available on the WWW under <http://www.eurjic.org> or from the author.



Scheme 1.



Scheme 2.



Scheme 3.

In order to systematically study how the steric bulk of the chelate affects the geometry of the assembled species, we have extended our investigation to bis(methylphenylglyoximate) complexes. These complexes exist both as *cis* and *trans* isomers due to the asymmetry of the equatorial ligand, and, when the axial ligands are different, the *trans* isomer is chiral. Therefore *trans*-[ $\text{CH}_3\text{Co}(\text{mpgH})\text{py}$ ] can be applied as a chiral building block in larger molecular systems.

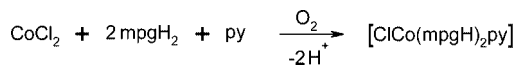
Here we report a study of the systems assembled from *trans*- and *cis*-[ $\text{CH}_3\text{Co}(\text{mpgH})\text{py}$ ] with 3- and 4- pyridylboronic acid, which includes the characterization of the dimeric aggregates formed both in solution and in the solid state and an investigation of their electrochemical properties.

## Results and Discussion

### Synthesis of the Organometallic Complexes

The ligand was prepared by addition of a tenfold excess of hydroxylamine hydrochloride, dissolved in water and neutralized with an equimolar amount of  $\text{NaOH}$ , to a methanolic solution of 1-phenyl-1,2-propanedione 2-oxime, as shown in Scheme 3.

[ $\text{ClCo}(\text{mpgH})_2\text{py}$ ] was prepared by direct air oxidation of  $\text{CoCl}_2$  in the presence of  $\text{mpgH}_2$  and pyridine (Scheme 4). The  $^1\text{H}$  NMR spectrum showed that the reaction product is a mixture of the *cis* and *trans* isomers.

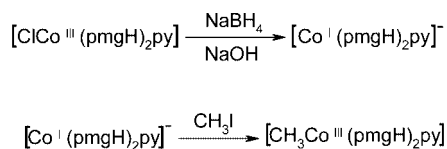


Scheme 4.

Small quantities of the pure isomers could be separated by stratification of *n*-heptane over a  $\text{CDCl}_3$  solution of the mixture in an NMR tube. After slow diffusion, two different kinds of crystals deposited on the walls of the tube and were manually separated. The  $^1\text{H}$  NMR spectrum in  $\text{CDCl}_3$  allowed identification of the *cis* and *trans* isomers, as the *cis* isomer gives rise to two singlets for the nonequivalent oximic protons, whereas only one signal is shown by the *trans* isomer. Integration of the signals of the equatorial methyls in the spectrum of the reaction mixture revealed that the *trans* isomer is the more abundant product of the synthesis. This isomer is chiral and exists in two enantiomeric forms.

The synthesis of the organometallic derivatives was carried out starting from the mixture of the *cis*- and *trans*-[ $\text{ClCo}(\text{mpgH})_2\text{py}$ ] isomers by reduction with  $\text{NaBH}_4$  followed by the oxidative addition of  $\text{CH}_3\text{I}$  (Scheme 5). The product always remained a mixture of isomers, but not nec-

essarily in the same ratio as in the starting mixture. *trans*-[CH<sub>3</sub>Co(mpgH)py] (**1**) and *cis*-[CH<sub>3</sub>Co(mpgH)py] (**2**) were separated by fractional crystallization from CH<sub>2</sub>Cl<sub>2</sub>/CH<sub>3</sub>OH (1:1) and characterized by <sup>1</sup>H NMR spectroscopy and X-ray structural analysis.



Scheme 5.

The chiral *trans* isomer was isolated as a racemic mixture of the A and C enantiomers.<sup>[12]</sup>

### Synthesis of the Supramolecular Species

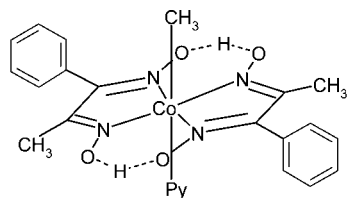
The reactions were performed in a mixture of solvents (chloroform/methanol, 1:6), because the starting complexes **1** and **2** are poorly soluble in methanol although a hydroxylic solvent is necessary for the formation of hydroxyboronate species containing a tetrahedral boron.<sup>[10b]</sup> X-ray quality crystals were obtained from solutions containing a racemic mixture of the *trans* derivative **1** and either 3-pyridylboronic acid (**3**) or 4-pyridylboronic acid (**4**). Small crystals, not of X-ray quality, were also obtained from the reactions of the *cis* isomer **2** with 3-pyridylboronic acid and 4-pyridylboronic acid (**5** and **6**, respectively) These were identified by ESI MS and <sup>1</sup>H NMR spectroscopy in noncoordinating solvents.

The formation of the supramolecular species from **1** was monitored in solution by <sup>1</sup>H NMR spectroscopy. When an equivalent amount of 3-(or 4-)pyridylboronic acid was added to the racemic mixture of *trans*-[CH<sub>3</sub>Co(mpgH)py] in CD<sub>3</sub>OD/CDCl<sub>3</sub> (1:1) at a pH of about 5, the <sup>1</sup>H NMR spectrum consisted of a complicated pattern of peaks, which did not simplify on standing for two weeks, attesting to the presence of several species besides **3** (or **4**; Figure S1). Removal of the solvent under vacuum yielded a mixture of products, which was not further characterized. However, if the solvent was left to evaporate slowly from the solution, the crystals deposited on the walls of the NMR tubes consisted of pure **3** (or **4**). Redissolution of **3** (or **4**) in CD<sub>3</sub>OD/CDCl<sub>3</sub> (1:1) resulted in a partial and slow decomposition of the supramolecular species (Figure S2).

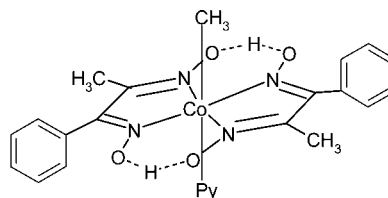
### X-ray Structures

ORTEP drawings of **1** and **2** are shown in Figure 1 together with their numbering scheme. Both **1** and **2** crystallize in a centrosymmetric space group with four molecules per unit cell. The equatorial ligand in **1** is nearly planar, the two dioximato moieties (excluding the phenyl side groups) making an interplanar angle of 1.9(3)°. The dioximato moieties in **2** are slightly bent towards the axial methyl group, making an interplanar angle of 6.2(1)°. The axial py ring is oriented with respect to the equatorial ligand in such a way as to nearly bisect the oxime bridges (orientation A) in **1**, whereas in **2** it is rotated by 17° towards N1 with respect to the orientation in **1**. No appreciable differences were detected in the coordination bond lengths and angles. Table 1 shows a comparison of the measured coordination distances with those reported for other methyl derivatives having different dioximate ligands. No evidence of a structural *cis*-influence is apparent.

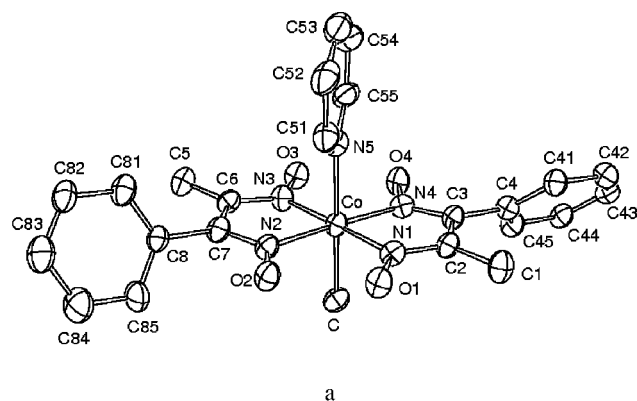
The crystal of **3** is built up by dimeric units arranged on a crystallographic symmetry center and methanol solvent. The dimeric unit (Figure 2a) is formed by two enantiomeric *trans*-[CH<sub>3</sub>Co(mpgH)<sub>2</sub>] moieties held together by two 3-pyridylboronic acid residues. This arrangement results in a *meso* species whose geometry is similar to that found in the analogous bis(dimethylglyoximate) derivative **3'**.<sup>[10a]</sup> The C–C<sub>Me</sub> and C–C<sub>Ph</sub> units are not coplanar, the C<sub>Me</sub> and C<sub>Ph</sub> atoms being about 0.2 Å out of the mean plane of the five-membered rings. In **3'**, the C–C<sub>Me</sub> bonds are nearly coplanar, with the C<sub>Me</sub> less than 0.1 Å out of the five-membered rings. The 3-pyridyl residue coordinated to the Co' atom is tilted by 167° (177° in **3'**) with respect to the equatorial plane, as measured by the Co'–N5–C22 angle. Thus, the two symmetry-related 3-py rings, which are essentially coplanar in **3'**, are still parallel in **3** but displaced by 1.45 Å. As a consequence, the “molecular parallelogram” in **3'** approaches a highly squeezed “molecular box” in **3**. Nevertheless, the dimensions of the Co···B···Co'···B' parallelogram in **3** are not significantly different from those in **3'**, with a decrease of more than 2° in the B···Co···B' angle (Table 1). As for **3'**, the 3-py mean plane in **3** is oriented in such a way as to nearly bisect the oxime bridge of the equatorial moiety (orientation A). The coordination bond lengths and angles do not differ significantly from those reported in **3'**. The axial Co–C and Co–N distances are compared in Table 1.



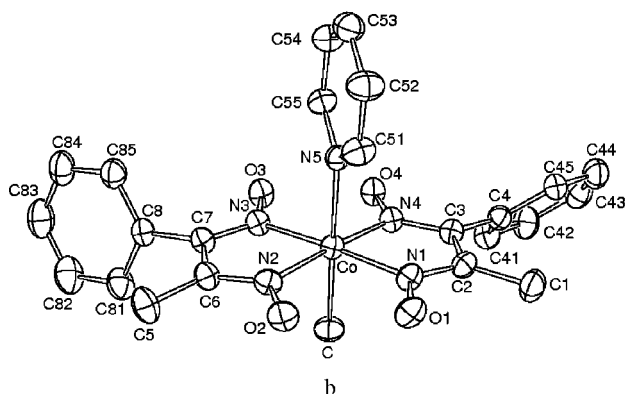
A enantiomer of **1**



C enantiomer of **1**



a



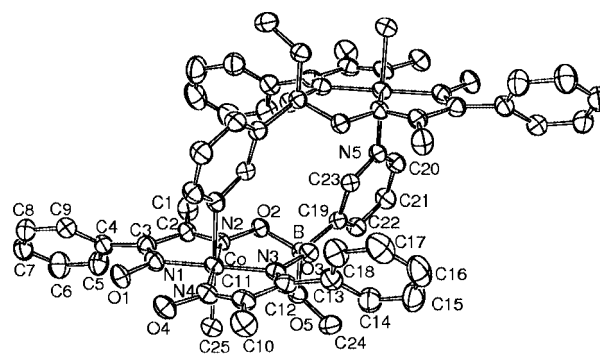
b

Figure 1. ORTEP drawing (thermal ellipsoids at 30% probability) and labeling scheme for **1** (a) and **2** (b).

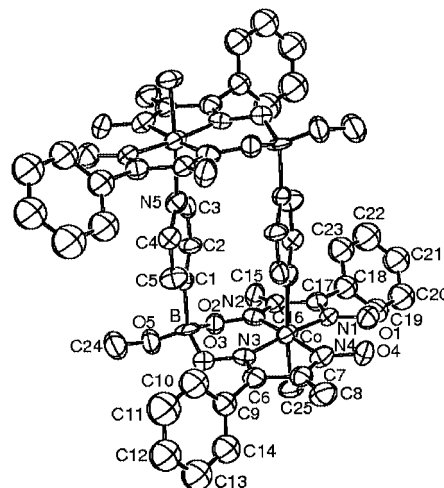
Table 1. Selected bond lengths [Å] of the mononuclear complexes **1** and **2** and the dinuclear complexes **3** and **4** compared with the corresponding distances for other methyl derivatives containing different dioximate ligands.

|   | Co–C     | Co–N     | Co–N <sub>eq</sub> (mean) |
|---|----------|----------|---------------------------|
| <b>1</b>  | 1.976(6) | 2.045(6) | 1.872(5)                  |
| <b>2</b>  | 1.994(4) | 2.057(3) | 1.882(3)                  |
| [CH <sub>3</sub> Co(dm <sub>g</sub> H) <sub>2</sub> py] <sup>[13]</sup> | 1.998(5) | 2.068(3) |                           |
| [CH <sub>3</sub> Co(dpgH) <sub>2</sub> py] <sup>[6b]</sup>              | 1.997(4) | 2.053(4) | 1.884(3)                  |
| <b>3</b>  | 2.003(3) | 2.074(3) | 1.875(3)                  |
| <b>3'</b> <sup>[10a]</sup>  | 1.985(9) | 2.069(8) | 1.869(8)                  |
| <b>4</b>  | 2.010(9) | 2.104(5) | 1.884(9)                  |
| <b>4'</b> <sup>[10b]</sup>  | 2.00(1)  | 2.08(1)  | 1.87(1)                   |
| <b>4''</b> <sup>[10c]</sup>   | 2.013(4) | 2.068(3) | 1.879(3)                  |

The crystal of **4** is built up by dimeric units arranged on a crystallographic symmetry center (ORTEP diagram in Figure 2b). The dimer is formed by two enantiomeric *trans*-[CH<sub>3</sub>Co(mpgH)<sub>2</sub>] moieties held together by two 4-pyridyl-boronic acid residues as for **3**. This arrangement results in a *meso* species whose geometry is very similar to those found in the analogous derivatives **4'**<sup>[10b]</sup> and **4''**<sup>[11]</sup> which contain dm<sub>g</sub>H and dpgH units, respectively. This result shows that the nature of the dioximate side substituents does not affect the geometry of such a dimeric arrangement (“molecular box”); the two symmetry-related 4-py rings face each other at an interplanar distance of about 3.4 Å.



a



b

Figure 2. ORTEP drawing (thermal ellipsoids at 30% probability) and labeling scheme for **3** (a) and **4** (b).

In all these dinuclear species, the axial 4-py ring nearly bisects the five-membered rings of the equatorial moiety (orientation B, rotated by about 90° with respect to orientation A found in **3** and **3'**). The resulting approximate Co⋯B⋯Co'⋯B' rectangle in **4** has Co⋯B and B'⋯Co' sides of 3.22 and 6.61 Å, respectively, and a B'⋯Co'⋯B' angle of 87.3°. A comparison with the corresponding figures in **4'**<sup>[10b]</sup> and **4''**<sup>[11]</sup> show that the side substituents in **4** lead to a more regular rectangle. The coordination bond lengths and angles do not differ appreciably from those found in **4'** and **4''**; the axial Co–C and Co–N distances are given in Table 1. A comparison of these data shows that the axial Co–N distances are not appreciably affected by the dioximate side substituents in either the mononuclear or in the series of dinuclear compounds. However, it seems that the Co–N<sub>ax</sub> distance (and possibly that of Co–C) is slightly lengthened in the dinuclear species.

#### Characterization of the Supramolecular Species in Solution

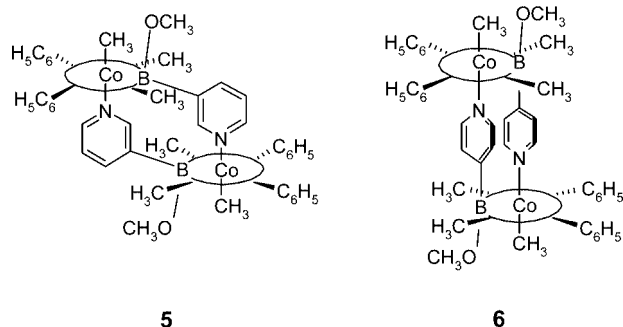
The ESI mass spectra of the supramolecular species **3**, **4**, **5**, and **6** in CH<sub>2</sub>Cl<sub>2</sub>/HCOOH (1%) show that the base peaks

for the molecular ions  $[M + H^+]$  correspond to protonated dimeric species held together by two pyridylboronic acids, with the residual  $B(OH)$  groups esterified by methanol.

The  $^1H$  NMR spectra of **3** and **4** in  $CDCl_3$  show similar features except for the signals of pyridine. Only one set of signals is evident, as a consequence of the presence of a symmetry center. The axial methyl, the  $B(OCH_3)$ , and the residual oximic protons give rise to three singlets, whereas the phenyl protons appear as a multiplet. The two singlets for the equatorial methyls confirm the insertion of a single boron bridge. The three py protons of **3** give rise to three signals in the range  $\delta = 7.25$ – $8.30$  ppm. The signal of the *ortho*  $NCHC(CH)B$  proton is notably shifted to lower field ( $\delta = 9.6$  ppm) with respect to the corresponding proton of free 3-pyridylboronic acid ( $\delta = 8.6$  ppm in  $CD_3OD$ ), due to the deshielding effect of the magnetic anisotropy of the parallel pyridyl ring. The pyridyl protons of **4** appear as four doublets in the range  $\delta = 6.72$ – $7.09$  ppm and are all non-equivalent as a consequence of the assembly and of the hindered rotation. The remarkable upfield shift of these protons with respect to the corresponding proton of the free 4-pyridylboronic acid ( $\delta = 8.05$  and  $8.47$  ppm in  $D_2O$ )<sup>[10b]</sup> is due to the shielding effect of the two facing pyridyl rings.

These results are entirely consistent with the solid-state structure, thereby suggesting that **3** and **4** are stable in solution in aprotic solvents – they neither dissociate nor are in equilibrium with species having different nuclearity.

The  $^1H$  NMR spectra of **5** and **6** in  $CDCl_3$  are very similar to those of **3** and **4**, respectively. The main differences are the presence of only one singlet for the equatorial methyls in both **5** and **6** and the internal equivalence of the *ortho* and the *meta* protons of pyridine in **6**. Both these results are consistent with the presence of a mirror plane bisecting the OHO and the OBO bridges. In the *cis* isomer **2**, the insertion of the boronic acid may occur either in the OHO bridge near to the methyl groups or in that near to the phenyl groups. The close proximity of the resonances of the equatorial methyl groups of **5** and **6** to the resonances of  $CH_3C=NOB$  in **3** and **4**, respectively, and the presence of a cross-peak between  $B(OCH_3)$  and the equatorial  $CH_3$  group in the ROESY spectrum, strongly support the former hypothesis. The proposed structures for **5** and **6**, very similar to those of **3** and **4**, are depicted in Scheme 6.



Scheme 6.

## Electrochemistry

The electrochemical behavior of both the mononuclear complexes **1** and **2** and the dinuclear species **3**–**6** was investigated by cyclic voltammetry in  $CH_2Cl_2$  containing 0.05 M tetra-*n*-butylammonium perchlorate (TBAP). This solvent proved to be suitably solubilizing for all the compounds and its conductivity is still sufficiently high to allow routine voltammetric studies.<sup>[14]</sup> This solvent-supporting electrolyte system allows a potential scan from +1.4 to  $-1.9$  V vs. SCE.

The behavior of the *trans*- and *cis*- $[CH_3Co(mpgH)_2py]$  isomers is very similar, so the following discussion refers equally to both derivatives. The CV of the mononuclear species **1** and **2** show three signals (Figure 3 and Table 2). The reduction peak **b** ( $E_{pc} = -1.625$  V in both cases, at  $100$   $mVs^{-1}$  scan rate) shifts toward more negative values at increasing scan rate and has no anodic counterpart up to  $1$   $Vs^{-1}$ . A further peak couple, **a** and **a'**, is visible at more positive potentials and is independent of the reduction peak **b**. In fact, it also develops if the CV is carried out in a range not including peak **b**, such as  $0$  V  $\rightarrow$   $+1.4$  V  $\rightarrow$   $0$  V. The linear dependence of the height of the peaks **a** and **a'** on the square root of the scan rate, the ratio between the cathodic and the anodic peak current,  $i_{pa}/i_{pc}$  (equal to 1), the constancy of  $(E_{pc} + E_{pa})/2$ , and the difference  $E_{pa} - E_{pc}$  (equal to  $110$  mV at  $100$   $mVs^{-1}$ ) all show that this peak couple corresponds to a quasi-reversible mono-electronic process.<sup>[15]</sup> This is assigned to a  $Co^{III}/Co^{IV}$  electron transfer in

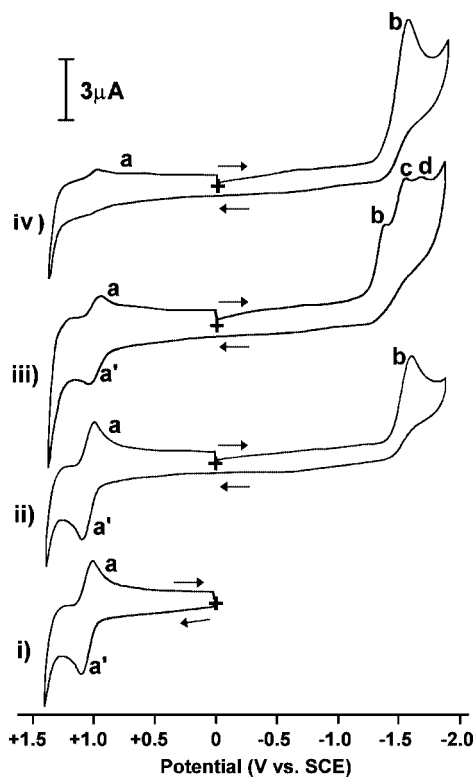


Figure 3. Cyclic voltammetry at a scan rate of  $100$   $mVs^{-1}$  in  $CH_2Cl_2$  + TBAP (0.05 M) at  $T = 0.0$  °C. i) and ii) complex **2**; iii) complex **5**; iv) complex **6**. Scans are made in the range 0 to  $+1.4$  V for i) and 0 to  $-1.9$  to  $+1.4$  V to 0 V for ii), iii) and iv).

which the oxidized species is stable in the CV time range.<sup>[16]</sup> On the basis of a comparison of the peak currents, the reduction peak **b** is attributed to a dielectronic Co<sup>III</sup>/Co<sup>I</sup> reduction, followed by a relatively fast chemical reaction, which gives no more electroactive species (EC mechanism).<sup>[15]</sup>

Table 2. Summary of  $E_p$  potentials at a scan rate of 100 mV s<sup>-1</sup> in CH<sub>2</sub>Cl<sub>2</sub> (TBAP 0.05 M) at 0.0 °C.

| Complex  | $E_{pa}(\mathbf{a})$ | $E_{pc}(\mathbf{a})$ | $E_{pc}(\mathbf{b})$ | $E_{pc}(\mathbf{c})$ | $E_{pc}(\mathbf{d})$ |
|----------|----------------------|----------------------|----------------------|----------------------|----------------------|
| <b>1</b> | +1.08                | +0.97                | -1.625               | –                    | –                    |
| <b>3</b> | +1.05 <sup>[a]</sup> | +0.95                | -1.57                | –                    | –                    |
| <b>4</b> | –                    | –                    | -1.41                | -1.60                | –                    |
| <b>2</b> | +1.09                | +0.98                | -1.625               | –                    | –                    |
| <b>5</b> | +1.05 <sup>[a]</sup> | +0.96                | -1.575               | –                    | –                    |
| <b>6</b> | +1.04                | +0.93                | -1.40                | -1.56                | -1.67                |

[a] Very low.

The cyclic voltammograms of the dinuclear species assembled with 3-pyridylboronic acid (**3** and **5**) show one cathodic signal **b** ( $E_{pc} = -1.57$  V in both cases at 100 mV s<sup>-1</sup>) without any anodic counterpart and a couple of low peaks **a** and **a'**, independent of the cathodic peak, at more positive potentials (Table 2 and Figure 3). The cyclic voltammograms of the dinuclear species assembled with 4-pyridylboronic acid (**4** and **6**) both show a couple of cathodic peaks that lack the anodic counterpart at 100 mV s<sup>-1</sup>:  $E_{pc}(\mathbf{b}) = -1.41$  and  $E_{pc}(\mathbf{c}) = -1.60$  V for **4** and  $E_{pc}(\mathbf{b}) = -1.40$  and  $E_{pc}(\mathbf{c}) = -1.56$  V for **6**. A very low and scarcely reproducible reduction peak **d** is present in the complex **6** at more negative value, but it was not investigated further. In addition, both species exhibit a further couple of peaks at more positive potential for both of them, but for complex **4** the signals are too low to determine the peak potential.

Therefore, in the dinuclear species, the chemically equivalent and noninteracting metal centers undergo the redox processes simultaneously at the same potential. It is noteworthy that, by comparison of the peak heights and the CV shape,<sup>[17]</sup> it is possible to attribute two consecutive two-electron reduction steps for **4** and **6** and a single four-electron reduction step for **3** and **5**. It has previously been reported that the electrochemical reduction of a series of organocobaloximes in aprotic solvents, such as dimethyl sulfide, dimethylformamide, and acetonitrile, takes place in two separate steps, but in pyridine or in the presence of strong donor species, a single two-electron step is observed.<sup>[18]</sup> In the present case, 3- and 4-pyridylboronic acids have very similar donor properties, but the orientation of the pyridyl ring in the dinuclear species is different. Indeed, the 3-pyridyl ring has the orientation A in **3** and **5**, whereas the 4-pyridyl ring has the orientation B in **4** and **6**. The latter orientation results in a lengthening of the Co–N bond (Table 1) and, in consequence, an apparent weakening of the electron-donor power of 4-pyridylboronic acid.

The reduction peak potentials of the monomers **1** and **2** are always more negative than that of the supramolecular species **3–6**. This behavior can be attributed to the stronger electron-donor power of pyridine with respect to the pyridylboronic acid due to the electron-withdrawing effect of the boron atom on the pyridyl ring.

## Conclusion

The reaction of racemic **1** with either 3- or 4-pyridylboronic acid can produce three structurally different dimeric species (two homodimers AA and CC and one heterodimer AC), but only the heterochiral dimers **3** (or **4**) crystallize from the reaction mixture. As the time-resolved <sup>1</sup>H NMR spectra of the reaction mixture do not show convergence toward a unique species in solution, the high enantiospecificity of the assembly has to be attributed to a preferential crystallization rather than to an enantiomeric self-recognition in solution.<sup>[19]</sup> Examples of preferential crystallization have been reported previously and have been attributed to an interplay of enthalpic, entropic, and crystal-packing factors.<sup>[20]</sup> Furthermore, both **3** and **4** are stable when dissolved in CDCl<sub>3</sub>/CD<sub>3</sub>OD, showing that the dissociation process in solution is quite slow. The slowness of both the formation and the dissociation process reflects the fact that the covalent O–B–O moiety has to be broken in this process.<sup>[21]</sup>

X-ray structural results show that the nature of the dioximate side substituents does not affect the geometry of the dimeric arrangements assembled by 4-pyridylboronic acid (“molecular box”). On the contrary, the geometry of the species assembled by 3-pyridylboronic acid varies from the “molecular parallelogram” obtained from the bis(dimethylglyoximates) to the highly squeezed “molecular box” obtained from methylphenylglyoximates.

Cyclic voltammetry studies show that the metal centers in the dimeric species do not interact with each other and undergo a simultaneous redox process. However, depending on the geometry of the systems, the redox process involves a single four-electron Co<sup>III</sup>/Co<sup>I</sup> step for **3** and **5** or two consecutive two-electron steps Co<sup>III</sup>/Co<sup>II</sup> and Co<sup>II</sup>/Co<sup>I</sup> for **4** and **6**.

## Experimental Section

**General Remarks:** <sup>1</sup>H NMR spectra were recorded with a Jeol EX-400 and referenced to residual solvent protons. Electrospray mass spectra were recorded in positive mode using an API 1 mass spectrometer (Perkin–Elmer). All reagents and solvents were obtained commercially and were used without further purification, unless otherwise stated.

**Electrochemical Measurements:** Cyclic voltammetry was performed with an Amel 551 potentiostat, equipped with positive feedback, driven by an Amel 568 function generator. The signals were recorded on an Amel 863 x-y recorder with a potential reproducibility of ±3 mV. A three-electrode system was used. The working electrode was a 2-mm-diameter glassy carbon disk (EG&G), which was polished with 0.3 and 0.05 micron Micropolish (Buehler) and sonicated in CH<sub>2</sub>Cl<sub>2</sub> solution before any measurement. The reference was an SCE (saturated NaCl) electrode, separated from the solution by a glass frit filled with a 0.05 M solution of TBAP (Fluka) in CH<sub>2</sub>Cl<sub>2</sub>. The counter electrode was a Pt wire. The mea-

measurements were performed on  $1 \times 10^{-3}$  M solutions of the complexes in  $\text{CH}_2\text{Cl}_2$  (Carlo Erba). The commercial solvent was shaken with  $\text{H}_2\text{SO}_4$ , water, and  $\text{NaHCO}_3$  (5% solution) and then distilled from  $\text{CaH}_2$  under argon. Dried TBAP (0.05 M) was used as supporting electrolyte. The temperature was maintained at  $0^\circ\text{C}$  and oxygen was removed by bubbling nitrogen that had first been pre-saturated with the solvent.

**Synthesis of the Ligand  $\text{mpgH}_2$ :** Hydroxylamine hydrochloride (21 g, 30 mmol) was dissolved in water (30 mL) and neutralized with an equimolar amount of NaOH. A methanolic solution of 1-phenyl-1,2-propanedione 2-oxime (5 g, 30 mmol in 80 mL) was added and the mixture was heated under reflux for 3 h. The precipitate was collected by filtration and washed with water and chloroform to give a white product. Yield: 4.25 g (78%).  $\text{C}_9\text{H}_{10}\text{N}_2\text{O}_2$  (178.19): calcd. C 60.7, H 5.66, N 15.7; found C 60.3, H 5.77, N 15.7. ESI-MS (60 V,  $\text{CH}_3\text{OH}$ ): calcd. for  $\text{mpgH}_2$  178.188; found 179.1 (100%).  $^1\text{H NMR}$  (400 MHz,  $[\text{D}_6]\text{DMSO}$ , TMS):  $\delta$  = 2.02 (s, 3 H,  $\text{CH}_3$ ), 7.14 (d,  $^3J_{\text{H,H}} = 8.3$  Hz, 2 H, *ortho* Ph), 7.20–7.43 (m, 3 H, *meta* and *para* Ph), 11.42 (s, 1 H,  $\text{CH}_3\text{C}=\text{NOH}$ ), 11.46 (s, 1 H,  $\text{PhC}=\text{NOH}$ ) ppm.

**Synthesis of  $[\text{ClCo}(\text{mpgH})_2\text{py}]$ :** The ligand  $\text{mpgH}_2$  (1.9 g, 11 mmol) was added to a suspension of  $\text{CoCl}_2 \cdot 6\text{H}_2\text{O}$  (1.3 g, 5.5 mmol) in ethanol (60 mL). The suspension was heated and stirred in the presence of air for 40 min. After the addition of py (0.9 mL, 11 mmol) to the resulting solution, the mixture was cooled to room temperature in a stream of air. After 2 h, a yellowish microcrystalline precipitate was collected by filtration. The  $^1\text{H NMR}$  spectrum showed that the precipitate was a mixture of the *cis* and *trans* isomers in a ratio of about 1:1.2. Yield: 2.07 g (71.3%).  $\text{C}_{23}\text{H}_{23}\text{ClCoN}_5\text{O}_4$  (527.85): calcd. C 52.3, H, 4.39, N 13.2; found C 52.8 H, 4.46, N 12.8. Small quantities of the isomers could be separated by stratification of *n*-heptane over a  $\text{CDCl}_3$  solution of the mixture in an NMR tube. After slow diffusion, two different kinds of crystals

deposited on the walls of the tube and were separated manually. The dark-brown crystals corresponded to the *trans* isomer, whereas the dark-yellow crystals corresponded to the *cis* isomer. ***trans*- $[\text{ClCo}(\text{mpgH})_2\text{py}]$ :**  $^1\text{H NMR}$  (400 MHz,  $\text{CDCl}_3$ , TMS):  $\delta$  = 2.32 (s, 6 H, equatorial  $\text{CH}_3$ ), 7.28 (m, 2 H, *meta* py), 7.45 (m, 10 H, equatorial phenyls), 7.75 (t,  $^3J_{\text{H,H}} = 7.6$  Hz, 1 H, *para* py), 8.42 (d,  $^3J_{\text{H,H}} = 5.2$  Hz, 2 H, *ortho* py), 18.07 (s, 2 H, *OHO*) ppm. ***cis*- $[\text{ClCo}(\text{mpgH})_2\text{py}]$ :**  $^1\text{H NMR}$  (400 MHz,  $\text{CDCl}_3$ , TMS):  $\delta$  = 2.34 (s, 6 H, equatorial  $\text{CH}_3$ ), 7.26 (m, 2 H, *meta* of py), 7.41 (m, 10 H, equatorial phenyls), 7.75 (t,  $^3J_{\text{H,H}} = 7.6$  Hz, 1 H, *para* of py), 8.4 (d,  $^3J_{\text{H,H}} = 5.6$  Hz, 2 H, *ortho* of py), 18.32 (s, 1 H, *OHO*), 18.52 (s, 1 H, *OHO*) ppm.

**Synthesis of  $[\text{CH}_3\text{Co}(\text{mpgH})_2\text{py}]$ :** NaOH (1 pellet in 2 mL of water) and a twofold excess of py (0.18 mL, 1.9 mmol) were added to a suspension of  $[\text{ClCo}(\text{mpgH})_2\text{py}]$  (mixture of *cis* and *trans* isomers in a ratio of 1:1.2; 0.50 g, 0.95 mmol) in 130 mL of methanol. The resulting solution was deaerated by bubbling nitrogen.  $\text{NaBH}_4$  (0.054 g, 1.42 mmol), dissolved in the minimum amount of water, and  $\text{CH}_3\text{I}$  (0.15 mL, 1.89 mmol) were then added in sequence. The solution was stirred at room temperature under nitrogen for 30 min and then the solvent was evaporated in vacuo. The orange crystals were collected by filtration. The  $^1\text{H NMR}$  spectrum showed that the precipitate was a mixture of the *cis* and *trans* isomers, in a ratio of about 1:1.2. The isomers were separated by fractional crystallization from  $\text{CH}_3\text{OH}/\text{CH}_2\text{Cl}_2$  (1:1), exploiting the lower solubility of the *trans* isomer. ***trans*- $[\text{CH}_3\text{Co}(\text{mpgH})_2\text{py}]$  (1):** Yield: 0.188 g (36%).  $\text{C}_{24}\text{H}_{26}\text{CoN}_5\text{O}_4$  (507.43): calcd. C 56.8, H 5.16, N 13.8; found C 55.7, H 5.06, N 13.6. ESI-MS (60 V,  $\text{MeOH}$ ): *m/z* calcd. for *trans*- $[\text{CH}_3\text{Co}(\text{mpgH})_2\text{py}]$  507.428; found 508.0 (60%); further peaks: *m/z* (%) = 530.0 (68)  $[\text{M} + \text{Na}^+]$ , 429.0 (96)  $[\text{M} - \text{py}]$ , 451.0 (100)  $[\text{M} + \text{Na}^+ - \text{py}]$ .  $^1\text{H NMR}$  (400 MHz,  $\text{CDCl}_3$ , TMS):  $\delta$  = 1.14 (s, 3 H, axial  $\text{CH}_3$ ), 2.05 (s, 6 H, equatorial  $\text{CH}_3$ ), 7.25–7.45 (m, 12 H, *meta* py and equatorial phenyls), 7.79 (t,  $^3J_{\text{H,H}} = 7.6$  Hz,

Table 3. Crystallographic data for 1–4.

|   | 1  | 2  | 3   | 4   |
|---|--|--|---|---|
| Empirical formula   | $\text{C}_{24}\text{H}_{26}\text{CoN}_5\text{O}_4$ | $\text{C}_{24}\text{H}_{26}\text{CoN}_5\text{O}_4$ | $\text{C}_{27}\text{H}_{35}\text{BCoN}_5\text{O}_7$ | $\text{C}_{25}\text{H}_{28}\text{BCoN}_5\text{O}_5$ |
| Formula mass  | 507.43   | 507.43   | 611.34  | 548.26  |
| Temperature [K]   | 200(2)   | 293(2)   | 150(2)  | 293(2)  |
| Wavelength [Å]  | 1.5418   | 0.71073  | 0.71073   | 1.5418  |
| Crystal system, S.G.                                      | monoclinic, $P2_1/c$                               | monoclinic, $P2_1/n$                               | monoclinic, $P2_1/n$                                | triclinic, $P\bar{1}$                               |
| <i>a</i> [Å]  | 14.497(4)  | 12.432(4)  | 10.216(3)   | 7.921(3)  |
| <i>b</i> [Å]  | 8.607(4)   | 15.442(4)  | 15.532(5)   | 11.777(3)   |
| <i>c</i> [Å]  | 19.140(6)  | 13.795(6)  | 18.584(5)   | 13.886(3)   |
| $\alpha$ [°]  | 90   | 90   | 90  | 104.92(2)   |
| $\beta$ [°]   | 100.10(3)  | 115.16(5)  | 92.26(2)  | 90.14(2)  |
| $\gamma$ [°]  | 90   | 90   | 90  | 94.36(2)  |
| Volume [Å <sup>3</sup> ]                                  | 2351.2(2)  | 2397.1(2)  | 2946.5(2)   | 1247.7(6)   |
| <i>Z</i> , $\rho_{\text{calcd}}$ [ $\text{Mg m}^{-3}$ ]   | 4, 1.433   | 4, 1.406   | 4, 1.378  | 2, 1.459  |
| $\mu$ [ $\text{mm}^{-1}$ ]                                | 6.066  | 0.756  | 0.635   | 5.785   |
| <i>F</i> (000)  | 1056   | 1056   | 1280  | 570   |
| Crystal size [mm]   | 0.3 × 0.2 × 0.1                                    | 0.3 × 0.3 × 0.3                                    | 0.5 × 0.3 × 0.3                                     | 0.2 × 0.1 × 0.1                                     |
| $\theta$ range for data collection [°]                    | 5.15 to 57.68                                      | 2.24 to 26.45                                      | 4.53 to 26.02                                       | 6.95 to 62.47                                       |
| Reflections unique/reflections with $I > 2\sigma(I)$      | 3108/2534  | 4930/3017  | 5756/4731   | 2248/1361   |
| Refinement method   | Full-matrix least squares on $F^2$                 | Full-matrix least squares on $F^2$                 | Full-matrix least squares on $F^2$                  | Full-matrix least squares on $F^2$                  |
| Data/restraints/parameters                                | 3108/0/310   | 4930/0/310   | 5756/0/356  | 2248/0/242  |
| Goodness-of-fit on $F^2$                                  | 0.896  | 0.714  | 1.066   | 0.756   |
| Final <i>R</i> indices [ $I > 2\sigma(I)$ ]               | $R_1 = 0.0693$<br>$wR_2 = 0.2020$                  | $R_1 = 0.0400$<br>$wR_2 = 0.1168$                  | $R_1^{[a]} = 0.0574$<br>$wR_2^{[b]} = 0.1551$       | $R_1 = 0.0849$<br>$wR_2 = 0.2006$                   |
| <i>R</i> indices (all data)                               | $R_1 = 0.0851$<br>$wR_2 = 0.2236$                  | $R_1 = 0.0772$<br>$wR_2 = 0.1508$                  | $R_1 = 0.0685$<br>$wR_2 = 0.1627$                   | $R_1 = 0.1332$<br>$wR_2 = 0.2383$                   |
| Largest difference peak/hole [ $\text{e} \text{Å}^{-3}$ ] | 0.315/−0.610                                       | 0.328/−0.456                                       | 1.036/−0.670  | 0.294/−0.336  |

[a]  $R_1 = \sum ||F_o| - |F_c|| / \sum |F_o|$ . [b]  $wR_2 = [\sum w(|F_o|^2 - |F_c|^2) / \sum w|F_o|^2]^{1/2}$ .

1 H, *para* py), 8.77 (d,  $^3J_{\text{H,H}} = 6.2$  Hz, 2 H, *ortho* py), 18.20 (s, 2 H, *OHO*) ppm. *cis*-[CH<sub>3</sub>Co(mpgH)<sub>2</sub>py] (**2**): Yield: 0.124 g (27%). C<sub>24</sub>H<sub>26</sub>CoN<sub>5</sub>O<sub>4</sub> (507.43): calcd. C 56.8, H, 5.16, N 13.8; found C 56.7, H 5.40, N 14.0. ESI-MS (60 V, MeOH): *m/z* calcd. for *cis*-[CH<sub>3</sub>Co(mpgH)<sub>2</sub>py] 507.428; found 508.0 (24%); further peaks: *m/z* (%) = 529.9 (28) [M + Na<sup>+</sup>], 429.1 (80) [M - py], 451.0 (100) [M + Na<sup>+</sup> - py]. <sup>1</sup>H NMR (400 MHz, CDCl<sub>3</sub>, TMS):  $\delta = 1.12$  (s, 3 H, axial CH<sub>3</sub>), 2.08 (s, 6 H, equatorial CH<sub>3</sub>), 7.25–7.42 (m, 12 H, *meta* of py and equatorial phenyls), 7.79 (t,  $^3J_{\text{H,H}} = 7.6$  Hz, 1 H, *para* of py), 8.75 (d,  $^3J_{\text{H,H}} = 6.2$  Hz, 2 H, *ortho* of py), 18.39 (s, 1 H, *OHO*), 18.56 (s, 1 H, *OHO*) ppm.

**Synthesis of 3:** A solution of 3-pyridylboronic acid (12 mg, 0.098 mmol in 6 mL of MeOH) was added to a solution of *trans*-[CH<sub>3</sub>Co(mpgH)<sub>2</sub>py] (0.050 g, 0.098 mmol in 1 mL CHCl<sub>3</sub>) The pH was adjusted to 5.5 with concentrated HClO<sub>4</sub> and NaOH. The solution was filtered and set aside in a beaker covered with Parafilm. After some days, small orange crystals of **3**, suitable for X-ray analysis, appeared and were collected by filtration. Yield: 33.2 mg (62%). C<sub>50</sub>H<sub>54</sub>B<sub>2</sub>Co<sub>2</sub>N<sub>10</sub>O<sub>10</sub> (1094.5): calcd. C 54.8, H 4.97, N 12.8; found C 55.3, H 5.10, N 12.7. ESI-MS (90 V, CH<sub>2</sub>Cl<sub>2</sub>/HCOOH 1%): *m/z* calcd. for **3** 1094.5; found 1095.4 (100%). <sup>1</sup>H NMR (400 MHz, CDCl<sub>3</sub>, TMS):  $\delta = 1.45$  (s, 6 H, axial CH<sub>3</sub>), 1.79 (s, 6 H, CH<sub>3</sub>C=NOH), 2.01 (s, 6 H, CH<sub>3</sub>C=NOB), 3.31 (s, 6 H, OCH<sub>3</sub>), 7.12–7.74 (m, 22 H, *meta* of py and equatorial phenyls), 7.90 (d,  $^3J_{\text{H,H}} = 6.8$  Hz, 2 H, *ortho* of py), 8.30 (d,  $^3J_{\text{H,H}} = 5.4$  Hz, 2 H, *para* of py), 9.60 (s, 2 H, *ortho* of py), 18.54 (s, 2 H, *OHO*) ppm.

**Synthesis of 4:** The synthesis was performed as described above using 4-pyridylboronic acid instead of 3-pyridylboronic acid. Yield: 17 mg (32%). C<sub>50</sub>H<sub>54</sub>B<sub>2</sub>Co<sub>2</sub>N<sub>10</sub>O<sub>10</sub> (1094.5): calcd. C 54.8, H 4.97, N 12.8; found C 54.3, H 5.03, N 12.3. ESI-MS (90 V, CH<sub>2</sub>Cl<sub>2</sub>/HCOOH 1%): *m/z* calcd. for **4** 1094.5; found 1095.4 (100%). <sup>1</sup>H NMR (400 MHz, CDCl<sub>3</sub>, TMS):  $\delta = 1.28$  (s, 6 H, axial CH<sub>3</sub>), 2.27 (s, 6 H, CH<sub>3</sub>C=NOH), 2.51 (s, 6 H, CH<sub>3</sub>C=NOB), 3.22 (s, 6 H, OCH<sub>3</sub>), 6.72(d,  $^3J_{\text{H,H}} = 5.4$  Hz, 2 H, *meta* of py), 6.83(d,  $^3J_{\text{H,H}} = 5.4$  Hz, 2 H, *meta* of py), 7.05 (d,  $^3J_{\text{H,H}} = 5.4$  Hz, 2 H, *ortho* of py), 7.09 (d,  $^3J_{\text{H,H}} = 5.4$  Hz, 2 H, *ortho* of py), 7.45–7.65 (m, 20 H, phenyls), 17.89 (s, 2 H, *OHO*) ppm.

**Synthesis of 5:** A solution of 3-pyridylboronic acid (12 mg, 0.098 mmol in 6 mL of MeOH) was added to a solution of *cis*-[CH<sub>3</sub>Co(mpgH)<sub>2</sub>py] (0.050 g, 0.098 mmol in 1 mL of CHCl<sub>3</sub>) and the pH was adjusted to 5.5. The solution was filtered and allowed to stand in a beaker covered with Parafilm for 2 d. Then, the solvent was evaporated under atmospheric pressure and the orange solid collected by filtration. Yield: 22.3 mg (41%). C<sub>50</sub>H<sub>54</sub>B<sub>2</sub>Co<sub>2</sub>N<sub>10</sub>O<sub>10</sub> (1094.5): calcd. C 54.8, H 4.97, N 12.8; found C 53.0, H 4.50, N 11.8. ESI-MS (90 V, CH<sub>2</sub>Cl<sub>2</sub>/HCOOH 1%): *m/z* calcd. for **5** 1094.5; found 1095.2 (100%). <sup>1</sup>H NMR (400 MHz, CDCl<sub>3</sub>, TMS):  $\delta = 1.49$  (s, 6 H, axial CH<sub>3</sub>), 1.99 (s, 12 H, CH<sub>3</sub>C=NOB), 3.44 (s, 6 H, OCH<sub>3</sub>), 7.30–7.50 (m, 22 H, *meta* of py and equatorial phenyls), 8.09 (d,  $^3J_{\text{H,H}} = 7.1$  Hz, 2 H, *ortho* of py), 8.46 (d,  $^3J_{\text{H,H}} = 5.5$  Hz, 2 H, *para* of py), 9.72 (s, 2 H, *ortho* of py), 18.56 (s, 2 H, *OHO*) ppm.

**Synthesis of 6:** A solution of 4-pyridylboronic acid (12 mg, 0.098 mmol in 6 mL of MeOH) was added to a solution of *cis*-[CH<sub>3</sub>Co(mpgH)<sub>2</sub>py] (0.050 g, 0.098 mmol in 1 mL of CHCl<sub>3</sub>) and the pH was adjusted to 5.5. The solution was filtered and allowed to stand in a beaker covered with Parafilm for 2 d. Then, two drops of water were added and the solvent evaporated under atmospheric pressure. The orange solid was collected by filtration. Yield: 6.3 mg (12%). C<sub>50</sub>H<sub>54</sub>B<sub>2</sub>Co<sub>2</sub>N<sub>10</sub>O<sub>10</sub> (1094.5): calcd. C 54.8, H 4.97, N 12.8; found C 53.8, H 5.41, N 11.7. ESI-MS (90 V, CH<sub>2</sub>Cl<sub>2</sub>/HCOOH 1%): *m/z* calcd. for **6** 1094.5; found 1095.4 (80%). <sup>1</sup>H NMR

(400 MHz, CDCl<sub>3</sub>, TMS):  $\delta = 1.28$  (s, 6 H, axial CH<sub>3</sub>), 2.53 (s, 12 H, CH<sub>3</sub>C=NOB), 3.37 (s, 6 H, OCH<sub>3</sub>), 6.84 (d,  $^3J_{\text{H,H}} = 6.3$  Hz, 4 H, *meta* of py), 7.16 (d,  $^3J_{\text{H,H}} = 6.3$  Hz, 4 H, *ortho* of py), 7.45–7.55 (m, 20 H, equatorial phenyls), 17.94 (s, 2 H, *OHO*) ppm.

**Structure Determinations:** Single crystals suitable for X-ray data collection were obtained as reported above. Data for the crystals of compounds **1** and **4**, being of small size and, in the case of **4**, also of poor quality, were collected at 200 K and 293 K, respectively, using a rotating copper-anode generator working at 45 kV and 95 mA, equipped with an Enraf Nonius KCCD diffractometer; 88 images for **1** and 176 for **4** were collected (crystal-to-detector distance of 42 mm) with 6° oscillation and 20 s° exposure time for CCD image. The data were processed, scaled, and merged with the programs DENZO and SCALE-PACK.<sup>[22]</sup> Data for the crystals of compounds **2** and **3** were collected at 293 K and 150 K, respectively, with a Nonius DIP 1030 H System, using graphite-monochromated Mo-*K $\alpha$*  radiation. For both compounds a total of 30 frames were collected using the Xpress program<sup>[23]</sup> over half of reciprocal space, with a rotation of 6° about the axis. A Mac Science Image Plate (diameter = 300 mm) was used and the crystal-to-plate distance was fixed at 90 mm. The determination of unit-cell parameters, integration of reflection intensities, and data scaling were performed using the programs DENZO and SCALE-PACK. All structures were solved by direct methods,<sup>[24]</sup> followed by Fourier syntheses and refined by full-matrix least squares (on *F*<sup>2</sup>) cycles.<sup>[25]</sup> The H atoms were not refined but were included at calculated positions in the final refinements. A suite of programs<sup>[26]</sup> was also used for the geometrical and final calculations. Crystal and refinement data are given in Table 3. CCDC-264667 to -264670 (**1–4**, respectively) contain the supplementary crystallographic data for this paper. These data can be obtained free of charge from The Cambridge Crystallographic Data Centre via [www.ccdc.cam.ac.uk/data\\_request/cif](http://www.ccdc.cam.ac.uk/data_request/cif).

**Supporting Information:** Time-resolved <sup>1</sup>H NMR spectra relative to the formation and decomposition of **3**, <sup>1</sup>H NMR spectra of **1–6**, and ESI mass spectra of **3–6**.

## Acknowledgments

This work was supported by MIUR (Prin 2003 no. 2003037580). P. S. acknowledges CIRCMSB (Consorzio Interuniversitario per la Ricerca sui Metalli nei Sistemi Biologici) for a grant. We thank Dr. Fabio Hollan for recording the mass spectra.

- a) N. Bresciani Pahor, M. Forcolin, L. G. Marzilli, L. Randaccio, M. F. Summers, P. J. Toscano, *Coord. Chem. Rev.* **1985**, *63*, 1; b) L. Randaccio, N. Bresciani Pahor, E. Zangrando, L. G. Marzilli, *Chem. Soc. Rev.* **1989**, *18*, 225; c) L. Randaccio, *Comments Inorg. Chem.* **1999**, *21*, 327.
- A. A. Gridner, S. D. Ittel, *Chem. Rev.* **2001**, *101*, 3611 and references cited therein.
- M. E. Welker, *Curr. Org. Chem.* **2001**, *5*, 785 and references cited therein.
- B. D. Gupta, R. Yamuna, V. Singh, U. Tiwari, *Organometallics* **2003**, *22*, 226 and references cited therein.
- B. D. Gupta, K. Qanungo, R. Yamuna, A. Pandey, U. Tiwari, V. Vijaikanth, V. Singh, T. Barclay, W. Cordes, *J. Organomet. Chem.* **2000**, *608*, 106 and references cited therein.
- a) P. J. Toscano, L. Lettko, E. Schermerhorn, J. Waechter, K. Schufon, S. Liu, E. V. Dikarev, J. Zubietta, *Polyhedron* **2003**, *22*, 2809; b) C. López, S. Alvarez, M. Font Bardía, X. Solans, *J. Organomet. Chem.* **1991**, *414*, 245; c) C. López, S. Alvarez, M. Aguiló, X. Solans, M. Font-Altaba, *Inorg. Chim. Acta* **1987**, *127*, 153; d) C. López, S. Alvarez, X. Solans, M. Font-Altaba,

- Inorg. Chem.* **1986**, *25*, 2962; e) B. D. Gupta, K. Qanungo, *J. Organomet. Chem.* **1997**, *543*, 125; f) B. D. Gupta, K. Qanungo, *J. Organomet. Chem.* **1998**, *560*, 155.
- [7] a) B. D. Gupta, V. Singh, K. Qanungo, V. Vijaikanth, R. Yamuna, T. Barclay, W. Cordes, *J. Organomet. Chem.* **2000**, *602*, 1; b) B. D. Gupta, R. Yamuna, V. Singh, U. Tiwari, T. Barclay, W. Cordes, *J. Organomet. Chem.* **2001**, *627*, 80; c) B. D. Gupta, U. Tiwari, T. Barclay, W. Cordes, *J. Organomet. Chem.* **2001**, *629*, 83.
- [8] a) Y. Ohgo, S. Takeuchi, *Chem. Lett.* **1985**, 407; b) A. Uchida, Y. Ohashi, Y. Sasada, Y. Ohgo, *Acta Crystallogr., Sect. C* **1985**, *41*, 25.
- [9] H. Höpfl, in *Structure & Bonding*, vol. 103 (Ed.: D. M. P. Mingos), Springer, Berlin, **2002**.
- [10] a) R. Dreos, G. Nardin, L. Randaccio, G. Tauzher, S. Vuano, *Inorg. Chem.* **1997**, *36*, 2463; b) R. Dreos, G. Nardin, L. Randaccio, P. Siega, G. Tauzher, V. Vrdoljak, *Inorg. Chem.* **2001**, *40*, 5536; c) R. Dreos, G. Nardin, L. Randaccio, P. Siega, G. Tauzher, *Eur. J. Inorg. Chem.* **2002**, 2885.
- [11] R. Dreos, G. Nardin, L. Randaccio, P. Siega, S. Scagliola, G. Tauzher, *Eur. J. Inorg. Chem.* **2004**, 4266.
- [12] The stereochemical description of the two enantiomers has been achieved by using the configuration index, the priming convention, and the chirality symbols based on the priority sequence (A/C stereochemical descriptors) [A. von Zelewski, *Stereochemistry of Coordination Compounds*; Wiley, Chichester, **1996**; J. G. Leigh, *Nomenclature of Inorganic Chemistry*, Blackwell, Oxford, **1990**]. For practical purposes, the C<sub>2</sub> axis of the molecule has been chosen as the reference axis with the view from py (having a lower priority number than CH<sub>3</sub>) to the metal atom. The complete stereochemical description of the C enantiomer is therefore OC-6-41'-C and that of the A enantiomer OC-6-41'-A.
- [13] A. Bigotto, E. Zangrando, L. Randaccio, *J. Chem. Soc., Dalton Trans.* **1976**, 96.
- [14] A. E. Kaifer, M. Gomez-Kaifer, *Supramolecular Electrochemistry*, Wiley-VCH, Weinheim, **1999**.
- [15] A. J. Bard, L. R. Faulkner, *Electrochemical Methods, Fundamentals and Applications*, John Wiley & Sons, Inc., New York, **1980**.
- [16] G. Costa, A. Puxeddu, C. Tavagnacco, R. Dreos-Garlatti, *Inorg. Chim. Acta* **1984**, *89*, 65 and references cited therein.
- [17] Due to the closeness of the background discharge to the reduction signals, it was not possible to obtain reproducible coulometric measurements of the number of electrons transferred.
- [18] a) G. Costa, A. Puxeddu, C. Tavagnacco, *J. Organomet. Chem.* **1985**, *296*, 161; b) C. Tavagnacco, G. Balducci, G. Costa, K. Täschler, W. von Philipsborn, *Helv. Chim. Acta* **1990**, *73*, 1469.
- [19] A. Wu, L. Isaacs, *J. Am. Chem. Soc.* **2003**, *125*, 4831 and references cited therein.
- [20] a) P. N. W. Baxter, J. M. Lehn, K. Rissanen, *Chem. Commun.* **1997**, 1323; b) Y. Yamanoi, Y. Sakamoto, T. Kusukawa, M. Fujita, S. Sakamoto, K. Yamaguchi, *J. Am. Chem. Soc.* **2001**, *123*, 980.
- [21] S. J. Rowan, S. J. Cantrill, G. R. L. Cousins, J. K. M. Sanders, J. F. Stoddart, *Angew. Chem. Int. Ed.* **2002**, *41*, 898.
- [22] Z. Otwinouski, W. Minor, *Methods Enzymol.* **1997**, *276*, 307.
- [23] a) B. Schierbeek, Nonius Delft The Netherlands, **1998**; b) Collaborative Computational Project, Number 4, *Acta Crystallogr. Sect. A* **1990**, *46*, 467.
- [24] *SIR92 – A program for crystal structure solution*: A. Altomare, G. Cascarano, C. Giacovazzo, A. Guagliardi, *J. Appl. Crystallogr.* **1993**, *26*, 343.
- [25] G. M. Sheldrick, *SHELXL-97 – Programs for Structure Refinement*, University of Göttingen, Göttingen, Germany, **1998**.
- [26] L. J. Farrugia, *J. Appl. Crystallogr.* **1999**, *32*, 837.

Received: February 28, 2005  
Published Online: August 4, 2005